Frustrated Lewis Pair Stabilized Phosphoryl Nitride (NPO), a Mono Phosphorus Analogue of Nitrous Oxide (N_2O)

André K. Eckhardt, Martin-Louis Y. Riu, Peter Müller and Christopher C. Cummins*

Department of Chemistry, Massachusetts Institute of Technology, Cambridge MA, USA; ccummins@mit.edu

Keywords: Azides – Frustrated Lewis Pairs – Photochemistry – Small Molecule Activation – Staudinger Reaction

Abstract. Phosphoryl nitride (NPO) is a highly reactive intermediate, and its chemistry has only been explored under matrix isolation conditions so far. Here we report the synthesis of an anthracene (**A**) and phosphoryl azide-based molecule ($N_3P(O)$**A**) that acts as a molecular synthon of NPO. Experimentally, $N_3P(O)$**A** dissociates thermally with a first order kinetic half-life that is associated with an activation enthalpy of $\Delta H^{\ddagger} = 27.5 \pm 0.3$ kcal mol^{-1} and an activation entropy of $\Delta S^{\ddagger} = 10.6 \pm 0.3$ cal mol^{-1} K^{-1} that are in good agreement with calculated DLPNO-CCSD(T)/cc-pVTZ//PBE0-D3(BJ)/cc-pVTZ energies. In solution $N_3P(O)$**A** undergoes Staudinger reactivity with tricyclohexylphosphine (PCy_3) and subsequent complexation with tris(pentafluorophenyl)borane ($B(C_6F_5)_3$, BCF) to form Cy_3P-NP(**A**)O-$B(C_6F_5)_3$. Anthracene is cleaved off photochemically to form the frustrated Lewis pair (FLP) stabilized NPO complex $Cy_3P^{\oplus}$-N=P-O-$B^{\ominus}(C_6F_5)_3$. Intrinsic Bond Orbital (IBO) analysis suggests that the adduct is zwitterionic, with a positive and negative charge localized on the complexing Cy_3P and BCF, respectively.

Phosphoryl nitride is the mono phosphorus analogue of well-known and studied nitrous oxide (N_2O), a naturally abundant gas that has been recognized as the dominant ozone-depleting substance in the Earth's stratosphere emitted in the 21st Century.[1] In chemical transformations N_2O is primarily used as a powerful oxidant, as it is a poor ligand to transition metals due to its weak σ-donating and π-accepting capabilities.[2] Nitrous oxide has been shown to coordinate to transition metal center in an end-on, as well as side-on, fashion.[3-11] Additionally, nitrous oxide easily forms stable complexes with frustrated Lewis pairs (FLPs) and N-heterocyclic carbenes (NHCs) under mild conditions.[12-14]

In contrast, little is known about the chemistry of linear two-fold coordinated phosphorus (V) NPO due to the lack of a suitable molecular precursor that releases the molecule under mild reaction conditions. Phosphoryl nitride was first generated 10 years ago via the irradiation of explosive phosphoryl triazide ($O{=}P(N_3)_3$)[15-17] and characterized under cryogenic matric isolation conditions.[18-19] Phosphoryl nitride undergoes photochemically induced isomerizations to PNO and cyclic PON (Figure 1) and reversibly combines with carbon monoxide.[18-19] On the other hand, the phosphorus(III) isomer PON has been known since 1988 and was formed after photolysis of an O_3/PN mixture diluted in solid argon under cryogenic matrix isolation conditions.[20] Interestingly, NPO was not observed in this experiment. In later experiments, namely gas-phase IR laser absorption spectroscopy of $NO/P_4/O_2$/noble-gas mixtures[21] and a microwave spectroscopic study of a dc glow discharge of NO/H_2 over red phosphorus,[22] there was also no experimental evidence for NPO. This is surprising given a recent high-level electronic structure focal point analysis suggesting that NPO is energetically preferred by 1.87 kcal mol^{-1} over PNO.[23] The Lewis structures of NPO and PNO are best described with formal charges rather than the neutral N≡P=O form (Figure 1).[18, 24-25] Related NPS isomers can be prepared in a similar fashion from thiophosphoryl azide ($S{=}P(N_3)_3$) via photolysis or high-vacuum flash pyrolysis (HVFP).[26] In the HVFP experiments the neutral five-membered sulfur–pnictogen(III) ring SN_2P_2 was also identified under the pyrolysis products, suggesting head-to-tail dimerization of SNP and subsequent elimination of a sulfur atom.[27] In the solid state, a material of the composition NPO is known to exist in both a β-cristobalite and a slightly thermodynamically less stable amorphous form.[28] Furthermore, isomers of NPO and NPS are also considered potential interstellar molecules,[18, 23-24] given the presence of PN in interstellar media.[29-30]

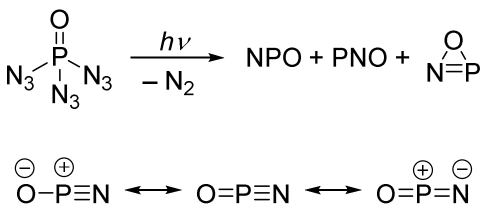

Figure 1: Top: Photochemical formation of all three NPO isomers. Bottom: Lewis structures of NPO.

Dibenzo-7λ^3-phosphanorbornadiene derivatives have served as suitable precursors to phosphorous bearing small molecules of interstellar interest.[31-34] We reported recently the synthesis of an anthracene-based azido phosphine (N_3P**A**) that releases molecular PN in solution and shown to transfer PN to an iron complex under mild conditions.[35] Here we report the oxidation of N_3P**A** to anthracene-based phosphoryl azide ($N_3P(O)$**A**, Figure 2). Given the poor thermal stability of N_3P**A** at room temperature ($t_{1/2}$ = 29.1 ± 1.6 min) we selected 2,4,6-trimethylbenzonitrile *N*-oxide (MesCNO) as a fast and effective oxygen atom transfer (OAT) reagent.[36] Inside the glovebox N_3P**A** and MesCNO were dissolved in a minimal amount of diethyl ether and tetrahydrofuran (4:1 ratio) and stirred under foil in the dark. After half an hour hexanes was added to the reaction mixture and the slurry was cooled to –20 °C to precipitate out the product. After half an hour the colorless precipitate was collected by vacuum filtration, washed with a minimal amount of pentane and dried under the nitrogen atmosphere of the glovebox providing up to 74% clean product. Single crystals of $N_3P(O)$**A** grown from diethyl ether at –20 °C were characterized in a single crystal X-ray diffraction experiment and the molecular structure is depicted in Figure 2 (see also Table S3). The structure is in line with strong infrared bands for the azide group at 2154 and 2141 cm^{-1} (Figure S4) as well as a single resonance in the ^{31}P NMR spectrum at δ 75.9 ppm (t, $^2J_{PH}$ = 11.1 Hz; Figure S3).

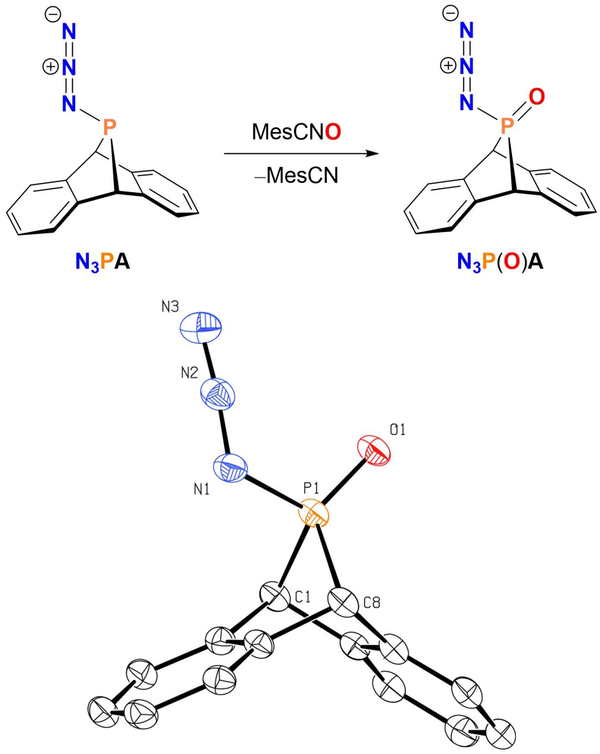

Figure 2: Top: Synthesis of $N_3P(O)$**A** using mesityl nitrile oxide (MesCNO) as an OAT reagent. Bottom: Molecular structure of $N_3P(O)$**A** with thermal ellipsoids shown at the 50% probability level. Hydrogen atoms are omitted for the sake of clarity. Selected interatomic distances (Å): P1−N1, 1.7066(17); P1−O1, 1.4754(13); P1−C1, 1.8520(19); P1−C8, 1.861(2); N1−N2, 1.243(2); and N2−N3, 1.128(3). Selected interatomic bond angles (°): C1−P1−C8, 83.51(9); N1–P1–O1, 111.61(8) and P1–N1–N2, 115.09(13).

$N_3P(O)$**A** was heated under vacuum and the release of molecules into the gas phase was monitored by mass spectrometry using a molecular-beam mass spectrometer (MBMS). We observed a strong increase in signals for N_2^+ (m/z = 28), P^+ (m/z = 31), PN^+ (m/z = 45), and **A**$^+$ (m/z = 178 and smaller fragments) starting at around 60 °C in the chromatogram. Additionally, a signal for m/z = 59 was observed that may originate from isomers of CPO^+ or PN_2^+. However, no signal at m/z = 61 for any NPO isomer was observed. Even reducing the voltage from 70 to 35 V in the electron impact ion source did not lead to the detection of any new signal for m/z = 61. Consistent with the observed decomposition at 60 °C in the MBMS experiment, solid $N_3P(O)$**A** melts at 45 °C and forms a red-brown solid at 60 °C.

In solution $N_3P(O)$**A** decomposes upon either thermal or photochemical activation. After 1 h irradiation of a quartz NMR tube containing a solution of $N_3P(O)$**A** in benzene-d_6 at λ = 254 nm only resonances of **A** could be detected in the ^{1}H NMR spectrum and no resonances were observed in the ^{31}P spectrum. Heating $N_3P(O)$**A** at 80 °C in benzene-d_6 for 30 min results in the observation of signals of **A** in the ^{1}H NMR spectrum as well as one major resonance at δ 112.7 ppm in the $^{31}P\{^1H\}$ spectrum together with some other minor resonances (Figure S5). However, none of these resonances could be unambiguously assigned. We followed the thermal decay of $N_3P(O)$**A** in benzene-d_6 by ^{1}H NMR spectroscopy (Figure S20-S22, Table S1-S2) and found that the azide decomposes at 52.5 °C with a first-order kinetics half-life of around half an hour ($t_{1/2}$ = 25.5 ± 0.4 min). Further kinetic measurements on $N_3P(O)$**A** decomposition were performed over the temperature range of 52.5–70.0 °C. An Eyring analysis revealed activation parameters of $\Delta H^‡$ = 27.5 ± 0.3 kcal mol^{-1} and $\Delta S^‡$ = 10.6 ± 0.3 cal mol^{-1} K^{-1} (Figure

S22). The first-order behavior is indicative of a unimolecular rate-determining step, consistent with fragmentation of $N_3P(O)$**A** into **A** and presumably a $O{=}PN_3$ fragment (*vide infra*).

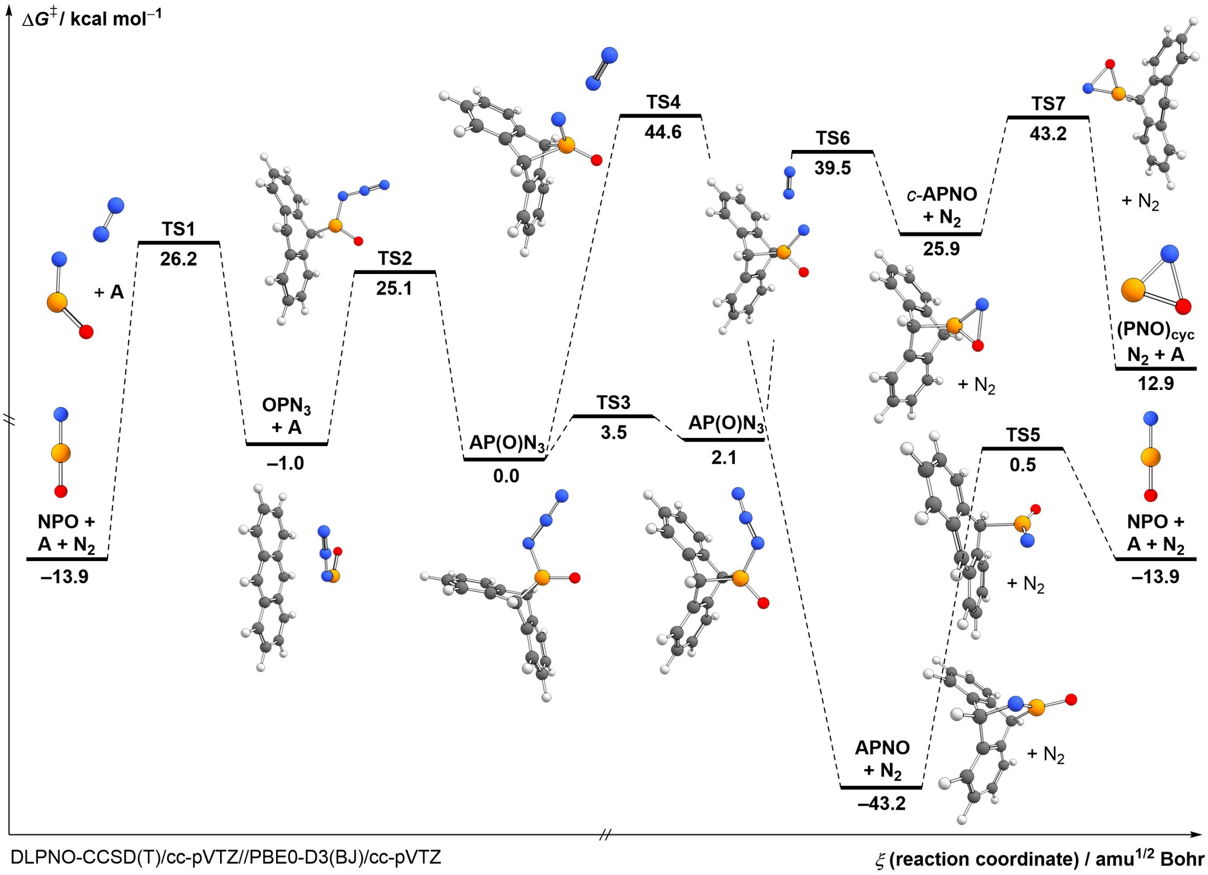

Figure 3: $N_3P(O)$**A** decomposes into N_2, cyclic and linear NPO isomers, and anthracene (**A**) either by dinitrogen and subsequent anthracene loss or via anthracene loss and further dissociation of the OPN_3 fragment into NPO and N_2. The latter pathway is energetically preferred. Gibbs free energy values are computed for $T = 298.15$ K. Color code: carbon = grey, hydrogen = white, nitrogen = blue, phosphorus = orange, oxygen = red.

We computed the most essential part of the potential energy surface around $N_3P(O)$**A** at PBE0-D3(BJ)/cc-pVTZ + Gibbs free energy correction with augmented DLPNO-CCSD(T)/cc-pVTZ single point energies (Figure 3). Similar as in our previous study of N_3P**A**,[35] we located two minima for $N_3P(O)$**A**, and the energetically preferred conformer is in line with our crystal structure depicted in Figure 2. In the higher energy conformer, the P–N single bond is rotated by 180° and the azide group takes a parallel position to a terminal aromatic ring that results in an energy rise of 2.1 kcal mol^{-1}. Both conformers are connected by a low lying transition state **TS3** (3.5 kcal mol^{-1}). For the fragmentation of $N_3P(O)$**A**, we initially considered cleavage of dinitrogen from the azide group. For each of the two $N_3P(O)$**A** conformers, we located, in contrast to N_3P**A**, an energetically high lying transition state (**TS4** (44.6 kcal mol^{-1}) and **TS6** (39.5 kcal mol^{-1})) that is associated with dinitrogen loss and a ring expansion to form tricyclic **A**PNO in a highly exothermic (–43.2 kcal mol^{-1}) and cyclic NPO attached to anthracene (*c*-**A**PNO) in a highly endothermic (25.9 kcal mol^{-1}) reaction, respectively. The dissociation reactions are completed with anthracene loss to form linear NPO via **TS5** (43.7 kcal mol^{-1} barrier) and cyclic NPO via **TS7** (17.3 kcal mol^{-1} barrier). However, in general these high reaction barriers cannot be overcome by simple heating at 80 °C. Therefore, we investigated a second dissociation pathway that is initiated by the cleavage of anthracene. We located a concerted transition state **TS2** that is associated with a reaction barrier of 25.2 kcal mol^{-1}, leading to the fragmentation of $N_3P(O)$**A** into **A** and OPN_3. These calculations also suggest that the latter fragment eliminates N_2 via **TS1** (26.2 kcal mol^{-1}) to form linear NPO. Based on the computed free energy values involving the elimination of **A** in the first step is energetically favored. The pathway via **TS2** with a total barrier of 25.1 kcal mol^{-1} is in good agreement with the experimental value of our Eyring analysis ($\Delta G^{\ddagger} = \Delta H^{\ddagger} - T\Delta S^{\ddagger}$ = 24.4 ± 0.1 kcal mol^{-1} at 298.15 K). However, the fate of the OPN_3 fragment remains unclear. The experimentally observed resonance at δ 112.7 ppm in the $^{31}P\{^1H\}$ after thermolysis cannot be assigned to the OPN_3 fragment or the NPO molecule.

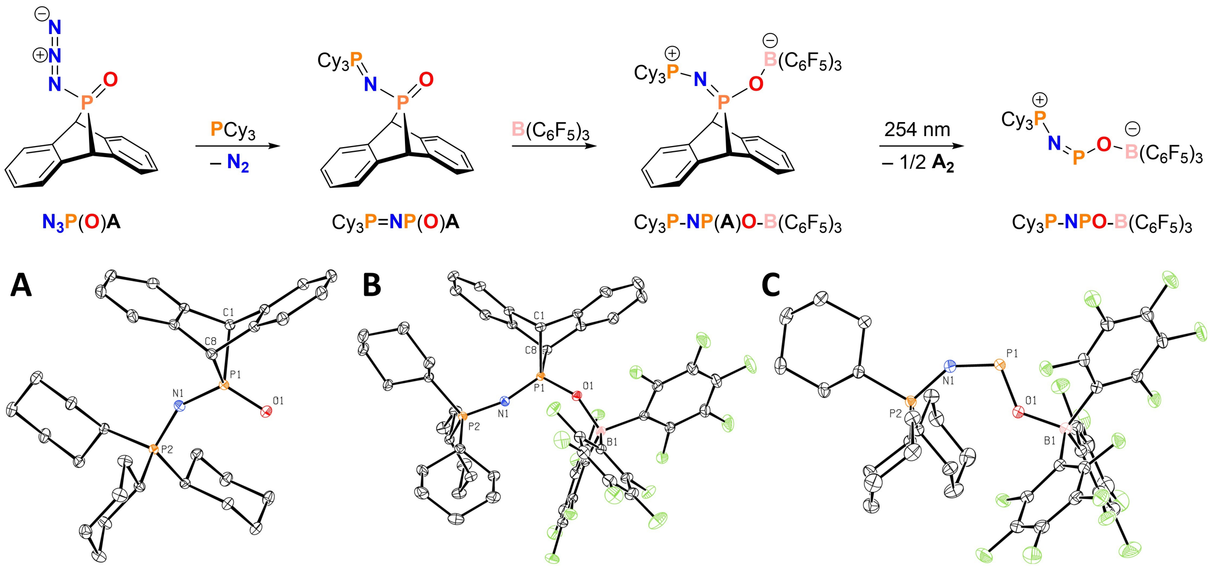

Figure 4: Top: Synthesis of $Cy_3P\text{-}NPO\text{-}B(C_6F_5)_3$. Bottom: Molecular structures of $Cy_3P{=}NP(O)$**A**, $Cy_3P\text{-}NP($**A**$)O\text{-}B(C_6F_5)_3$ and $Cy_3P\text{-}NPO\text{-}B(C_6F_5)_3$ with thermal ellipsoids shown at the 50% probability level. Hydrogen atoms are omitted for the sake of clarity. Selected interatomic distances (Å) and bond angles (°): **A**: $(Cy_3)P{-}N$, 1.5765(8); N−P, 1.5813(9) and P−O, 1.4889(8); $(Cy_3)P{-}N{-}P$, 147.62(6) and N–P–O, 119.59(4). **B**: $(Cy_3)P{-}N$, 1.5761(12); N−P, 1.5465(12); P−O, 1.5171(10) and O−B, 1.5110(18); $(Cy_3)P{-}N{-}P$, 165.17(9); N–P–O, 114.43(6) and P–O–B, 148.83(9); **C**: $(Cy_3)P{-}N$, 1.6289(9); N−P, 1.5555(9); P−O, 1.5549(8) and O−B, 1.5454(13); $(Cy_3)P{-}N{-}P$, 140.18(6); N–P–O, 110.73(4) and P–O–B, 131.50(6).

Schulz and co-workers reported on the Staudinger reactivity[37] of $S{=}P(N_3)_3$ with triphenylphosphine (PPh_3), which led to the single ($S{=}P(N_3)_2NPPh_3$) and double ($S{=}P(N_3)(NPPh_3)_2$) but not the triple (($S{=}P(NPPh_3)_3$)) Staudinger products.[38] Inspired by this work, we treated $N_3P(O)$**A** with PPh_3 at room temperature; however, no reaction was observed. This reaction was repeated with the more electron-rich tricyclohexylphosphine (PCy_3) in diethyl ether and immediate gas evolution and precipitation of the Staudinger reaction product $Cy_3P{=}NP(O)$**A** was observed (Figure 4). The product was isolated by vacuum filtration in 82% yield (Figure S6-S8). $Cy_3P{=}NP(O)$**A** exhibits two doublets at δ 82.9 and δ 32.3 ($^2J_{PP}$ = 21.4 Hz) in the $^{31}P\{^1H\}$ NMR spectrum (Figure S8). Additionally, $Cy_3P{=}NP(O)$**A** was characterized in a single crystal X-ray diffraction experiment and the molecular structure is depicted in Figure 4A.

Considering that nitrous oxide[12] and many other small molecules have already been reported to form complexes with frustrated Lewis pairs (FLPs),[39-40] we added tris(pentafluorophenyl)borane ($B(C_6F_5)_3$, BCF) to a solution of $Cy_3P{=}NP(O)$**A** in dichloromethane, leading to new ^{31}P NMR resonances at δ 52.5 and δ 32.9 ($^2J_{PP}$ = 16.8 Hz) in the $^{31}P\{^1H\}$ NMR spectrum (Figure S11). After the reaction mixture stirred for 30 min at room temperature, all volatile materials were removed under reduced pressure, allowing us to isolate

Cy_3P–NP(**A**)O–B(C_6F_5)$_3$ as a colorless solid in quantitative yield (Figure S9-S13). An analytical sample was crystallized in diethyl ether and the crystals were analyzed in a X-ray diffraction experiment, leading to the structure depicted in Figure 4B. For the complete complexation of NPO, **A** can be cleaved off by irradiating (λ = 254 nm) a solution of Cy_3P-NP(**A**)O-B(C_6F_5)$_3$ in benzene or toluene for 220 min. Anthracene photodimerizes during the irradiation and can separated from the reaction mixture by filtration.[41] The slightly yellow colored filtrate was mixed (in the case of benzene as a solvent) or layered with pentane and placed in the freezer. After three days colorless crystals formed and the crystals were collected by vacuum filtration, washed with pentane and isolated in 42% yield (Figure S14-S18). When the isolated material was dissolved in chloroform a doublet signal at δ 44.1 (J = 78.2 Hz) for PCy_3 and a doublet of quintets signal at δ 271.1 ppm (J = 77.4, 25.5 Hz) for NPO were observed in the $^{31}P\{^1H\}$ NMR spectrum (Figure S16). X-ray diffraction analysis on a single crystal directly grown from a benzene/pentane solution after irradiation reveals the Cy_3P-NPO-B(C_6F_5)$_3$ structure (Figure 4C). The latter splitting originates from through space coupling of phosphorus to fluorine in B(C_6F_5)$_3$ as only a doublet signal is observed in the $^{31}P\{^1H, ^{19}F\}$ NMR experiment.[42] The compound is thermally unstable and decomposes after one day at room temperature or by heating over night at 50 °C. In the $^{31}P\{^1H\}$ NMR spectrum, two major doublet signals at δ 42.2 and δ 40.7 ppm together with some minor signals at around δ –20 ppm were observed that could not be unambiguously assigned (Figure S19).

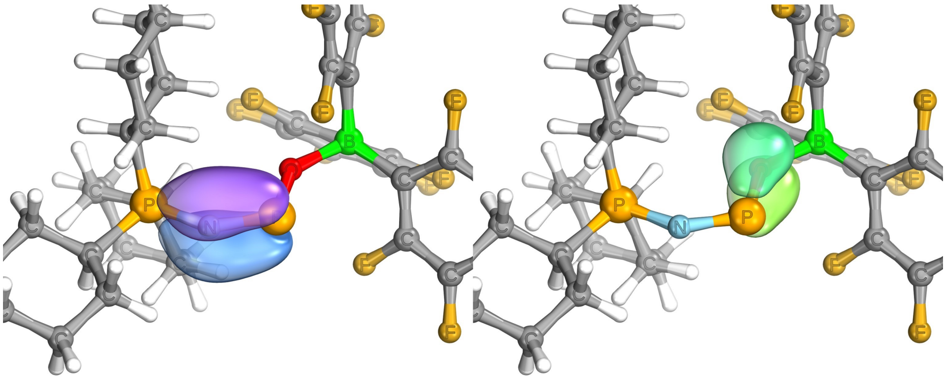

Figure 5: Computed Intrinsic Bond Orbitals (IBOs) of the N-P (left) and P-O (right) π-bonds based on the geometry of the X-ray structure depicted in Figure 4C at ωB97M-D3(BJ)/def2-TZVPP.

The interatomic distances in the single crystal for the NPO fragment are almost the same for the N−P (1.5555(9) Å) and P−O (1.5549(8) Å) linkages. Intrinsic Bond Orbital (IBO) analysis shows the bonding of the π system, where there is visual evidence for both N−P and P−O π bonding (Figure 5). The Wiberg bond order (WBO) for the N-P bond is 1.47 and for the P−O bond 1.05. The bond orders are reflective of the high electronegativity of N and O and the consequent greater coefficients on N and O rather than P in the π system, which acts to bring down the WBO numbers. Hence, the main resonance contributor is the one with the $Cy_3P^{\oplus}$-N=P-O-$B^{\ominus}$(C_6F_5)$_3$ bonding pattern, and formal positive and negative charges on the phosphine and borate, respectively. Compounds of the type R-N=P-OR' exhibit a similar bonding pattern, but they are rare and mainly derive from the combination of an alkoxide with the Mes*NP+ cation.[43-50] Gaseous NPO is predicted to be linear, and has two bonds of almost equal length, a N–P bond distance of 1.4965Å at the CCSD(T)/CBS level and a P–O bond distance of 1.4656Å at the same level.[24] Similar to N_2O, the geometry of NPO is bent in its FLP complex.

Data Availability

All relevant data generated and analyzed during this study, including crystal structures, NMR, IR, MBMS spectra and optimized coordinates for all calculated compounds, are included in this Article and its Supplementary Information, and are also available from the authors upon reasonable request.

Acknowledgements

A.K.E. thanks the Alexander von Humboldt foundation for a Feodor Lynen postdoctoral fellowship. This material is based on research supported by the National Science Foundation, under No. CHE-1955612.

Competing financial interests

None.

Materials & Correspondence

Correspondence and material requests should be addressed to C.C.C.

Orcid

A.K.E. 0000-0003-1029-9272
M.L.Y.R. 0000-0002-0900-3545
P.M. 0000-0001-6530-3852
C.C.C. 0000-0003-2568-3269

References

1. Ravishankara, A.; Daniel, J. S.; Portmann, R. W., Nitrous oxide (N_2O): the dominant ozone-depleting substance emitted in the 21st century. *Science* **2009,** *326*, 123-125.
2. Severin, K., Synthetic chemistry with nitrous oxide. *Chem. Soc. Rev.* **2015,** *44*, 6375-6386.
3. Armor, J. N.; Taube, H., Formation and reactions of $[(NH_3)_5RuN_2O^{2+}]$. *J. Am. Chem. Soc.* **1969,** *91*, 6874-6876.
4. Bottomley, F.; Brooks, W. V. F., Mode of bonding of dinitrogen oxide (nitrous oxide) in (dinitrogen oxide)pentaammineruthenium. *Inorg. Chem.* **1977,** *16*, 501-502.
5. Paulat, F.; Kuschel, T.; Näther, C.; Praneeth, V. K. K.; Sander, O.; Lehnert, N., Spectroscopic Properties and Electronic Structure of Pentammineruthenium(II) Dinitrogen Oxide and Corresponding Nitrosyl Complexes: Binding Mode of N_2O and Reactivity. *Inorg. Chem.* **2004,** *43*, 6979-6994.
6. Pamplin, C. B.; Ma, E. S. F.; Safari, N.; Rettig, S. J.; James, B. R., The Nitrous Oxide Complex, $RuCl_2(\eta^1\text{-}N_2O)(P{-}N)(PPh_3)$ (P−N = [*o*-(*N*,*N*-Dimethylamino)phenyl]diphenylphosphine); Low Temperature Conversion of N_2O to N_2 and O_2. *J. Am. Chem. Soc.* **2001,** *123*, 8596-8597.
7. Piro, N. A.; Lichterman, M. F.; Harman, W. H.; Chang, C. J., A Structurally Characterized Nitrous Oxide Complex of Vanadium. *J. Am. Chem. Soc.* **2011,** *133*, 2108-2111.
8. Gyton, M. R.; Leforestier, B.; Chaplin, A. B., Rhodium(I) Pincer Complexes of Nitrous Oxide. *Angew. Chem. Int. Ed.* **2019,** *58*, 15295-15298.

9. Zhuravlev, V.; Malinowski, P. J., A Stable Crystalline Copper(I)–N_2O Complex Stabilized as the Salt of a Weakly Coordinating Anion. *Angew. Chem. Int. Ed.* **2018,** *57*, 11697-11700.
10. Mokhtarzadeh, C. C.; Chan, C.; Moore, C. E.; Rheingold, A. L.; Figueroa, J. S., Side-On Coordination of Nitrous Oxide to a Mononuclear Cobalt Center. *J. Am. Chem. Soc.* **2019,** *141*, 15003-15007.
11. Puerta Lombardi, B. M.; Gendy, C.; Gelfand, B. S.; Bernard, G. M.; Wasylishen, R. E.; Tuononen, H. M.; Roesler, R., Side-on Coordination in Isostructural Nitrous Oxide and Carbon Dioxide Complexes of Nickel. *Angew. Chem. Int. Ed.* **2021,** *60*, 7077-7081.
12. Otten, E.; Neu, R. C.; Stephan, D. W., Complexation of Nitrous Oxide by Frustrated Lewis Pairs. *J. Am. Chem. Soc.* **2009,** *131*, 9918-9919.
13. Tskhovrebov, A. G.; Solari, E.; Wodrich, M. D.; Scopelliti, R.; Severin, K., Covalent Capture of Nitrous Oxide by N-Heterocyclic Carbenes. *Angew. Chem. Int. Ed.* **2012,** *51*, 232-234.
14. Tskhovrebov, A. G.; Vuichoud, B.; Solari, E.; Scopelliti, R.; Severin, K., Adducts of Nitrous Oxide and N-Heterocyclic Carbenes: Syntheses, Structures, and Reactivity. *J. Am. Chem. Soc.* **2013,** *135*, 9486-9492.
15. Dillon, K. B.; Platt, A. W. G.; Waddington, T. C., The identification of some new azido-derivatives of phosphorus. *Inorg. Nucl. Chem. Letters* **1978,** *14*, 511-513.
16. Buder, W.; Schmidt, A., Phosphorazide und deren Schwingungsspektren. *Z. Anorg. Allg. Chem.* **1975,** *415*, 263-267.
17. Zeng, X.; Bernhardt, E.; Beckers, H.; Willner, H., Synthesis and Characterization of the Phosphorus Triazides $OP(N_3)_3$ and $SP(N_3)_3$. *Inorg. Chem.* **2011,** *50*, 11235-11241.
18. Zeng, X.; Beckers, H.; Willner, H., Elusive O═P≡N, a Rare Example of Phosphorus $\sigma^2\lambda^5$-Coordination. *J. Am. Chem. Soc.* **2011,** *133*, 20696-20699.
19. Wu, Z.; Song, C.; Liu, J.; Lu, B.; Lu, Y.; Trabelsi, T.; Francisco, J. S.; Zeng, X., Photochemistry of OPN: Formation of Cyclic PON and Reversible Combination with Carbon Monoxide. *Chem. Eur. J.* **2018,** *24*, 14627-14630.
20. Ahlrichs, R.; Schunck, S.; Schnöckel, H., Structure of Molecular PNO, Matrix Isolation and ab initio Calculations. *Angew. Chem. Int. Ed.* **1988,** *27*, 421-423.
21. Bell, I. S.; Hamilton, P. A.; Davies, P. B., Detection of the transient PNO molecule by infrared laser absorption spectroscopy. *Mol. Phys.* **1998,** *94*, 685-691.
22. Okabayashi, T.; Yamazaki, E.; Tanimoto, M., Microwave spectrum and molecular structure of PNO. *J. Chem. Phys.* **1999,** *111*, 3012-3017.
23. Turner, W. E.; Agarwal, J.; Schaefer, H. F., Structures, Bonding, and Energetics of Potential Triatomic Circumstellar Molecules Containing Group 15 and 16 Elements. *J. Phys. Chem. A* **2015,** *119*, 11693-11700.
24. Grant, D. J.; Dixon, D. A.; Kemeny, A. E.; Francisco, J. S., Structures and heats of formation of the neutral and ionic PNO, NOP, and NPO systems from electronic structure calculations. *J. Chem. Phys.* **2008,** *128*, 164305.
25. Himmel, H.-J.; Linti, G., OPN and SPN: Small Molecules with Great Potential. *Angew. Chem. Int. Ed.* **2012,** *51*, 5541-5542.
26. Zeng, X.; Beckers, H.; Willner, H.; Francisco, J. S., Experimental Observation of the 16-Electron Molecules SPN, SNP, and Cyclic PSN. *Angew. Chem. Int. Ed.* **2012,** *51*, 3334-3339.
27. Zeng, X.; Li, H.; Sun, H.; Beckers, H.; Willner, H.; Schaefer Iii, H. F., SN_2P_2: A Neutral Five-Membered Sulfur–Pnictogen(III) Ring. *Angew. Chem. Int. Ed.* **2015,** *54*, 1327-1330.
28. Tessier, F.; Navrotsky, A.; Le Sauze, A.; Marchand, R., Thermochemistry of Phosphorus Oxynitrides: PON and LiNaPON Glasses. *Chem. Mater.* **2000,** *12*, 148-154.
29. Ziurys, L., Detection of interstellar PN-the first phosphorus-bearing species observed in molecular clouds. *Astrophys. J.* **1987,** *321*, L81-L85.
30. Turner, B.; Bally, J., Detection of interstellar PN-The first identified phosphorus compound in the interstellar medium. *Astrophys. J.* **1987,** *321*, L75-L79.
31. Velian, A.; Cummins, C. C., Facile Synthesis of Dibenzo-7λ^3-phosphanorbornadiene Derivatives Using Magnesium Anthracene. *J. Am. Chem. Soc.* **2012,** *134*, 13978-13981.
32. Velian, A.; Nava, M.; Temprado, M.; Zhou, Y.; Field, R. W.; Cummins, C. C., A Retro Diels–Alder Route to Diphosphorus Chemistry: Molecular Precursor Synthesis, Kinetics of P_2 Transfer to 1,3-Dienes, and Detection of P_2 by Molecular Beam Mass Spectrometry. *J. Am. Chem. Soc.* **2014,** *136*, 13586-13589.

33. Transue, W. J.; Velian, A.; Nava, M.; Martin-Drumel, M.-A.; Womack, C. C.; Jiang, J.; Hou, G.-L.; Wang, X.-B.; McCarthy, M. C.; Field, R. W.; Cummins, C. C., A Molecular Precursor to Phosphaethyne and Its Application in Synthesis of the Aromatic 1,2,3,4-Phosphatriazolate Anion. *J. Am. Chem. Soc.* **2016,** *138*, 6731-6734.
34. Transue, W. J.; Nava, M.; Terban, M. W.; Yang, J.; Greenberg, M. W.; Wu, G.; Foreman, E. S.; Mustoe, C. L.; Kennepohl, P.; Owen, J. S.; Billinge, S. J. L.; Kulik, H. J.; Cummins, C. C., Anthracene as a Launchpad for a Phosphinidene Sulfide and for Generation of a Phosphorus–Sulfur Material Having the Composition P_2S, a Vulcanized Red Phosphorus That Is Yellow. *J. Am. Chem. Soc.* **2019,** *141*, 431-440.
35. Eckhardt, A. K.; Riu, M.-L. Y.; Müller, P.; Cummins, C. C., Taming Phosphorus Mononitride (PN). *Preprint on ChemRxiV* **2021**, doi:10.33774/chemrxiv-32021-zxtmf.
36. Palluccio, T. D.; Rybak-Akimova, E. V.; Majumdar, S.; Cai, X.; Chui, M.; Temprado, M.; Silvia, J. S.; Cozzolino, A. F.; Tofan, D.; Velian, A.; Cummins, C. C.; Captain, B.; Hoff, C. D., Thermodynamic and Kinetic Study of Cleavage of the N–O Bond of N-Oxides by a Vanadium(III) Complex: Enhanced Oxygen Atom Transfer Reaction Rates for Adducts of Nitrous Oxide and Mesityl Nitrile Oxide. *J. Am. Chem. Soc.* **2013,** *135*, 11357-11372.
37. Staudinger, H.; Meyer, J., Über neue organische Phosphorverbindungen III. Phosphinmethylenderivate und Phosphinimine. *Helv. Chim. Acta* **1919,** *2*, 635-646.
38. Götz, N.; Herler, S.; Mayer, P.; Schulz, A.; Villinger, A.; Weigand, J. J., On the Staudinger Reaction of $SP(N_3)_3$ with PPh_3 and$(Me_3Si)_2N–(Me_3Si)N–PPh_2$. *Eur. J. Inorg. Chem.* **2006,** *2006*, 2051-2057.
39. Stephan, D. W.; Erker, G., Frustrated Lewis Pair Chemistry: Development and Perspectives. *Angew. Chem. Int. Ed.* **2015,** *54*, 6400-6441.
40. Jupp, A. R.; Stephan, D. W., New Directions for Frustrated Lewis Pair Chemistry. *Trends Chem.* **2019,** *1*, 35-48.
41. Bouas-Laurent, H.; Castellan, A.; Desvergne, J.-P.; Lapouyade, R., Photodimerization of anthracenes in fluid solution: structural aspects. *Chem. Soc. Rev.* **2000,** *29*, 43-55.
42. Beckett, M. A.; Tebby, J. C.; Thompson, J. J.; Williams, B. J.; Withington, S. C., Phosphorus-31 Fluorine-19 N.M.R. Through-Space Coupling. *Phosphorus Sulfur Silicon Relat. Elem.* **1990,** *51*, 277-277.
43. Chernega, A. I.; Antipin, M. Y.; Struchkov, Y. T.; Ruban, A. V.; Romanenko, V. D., The structure of organophosphorus compounds. Part XLIV. The molecular structure of the 2-methylphenyl ester of *N*-[2, 4, 6-tri(*tert*-butyl) phenyl] imidophosphenous acid. *J. Struct. Chem.* **1990,** *31*, 301-306.
44. Niecke, E.; Detsch, R.; Nieger, M.; Reichert, F.; Schoeller, W., From covalent to ionic bonding: spontaneous bond dissociation in oxy-substituted iminophosphanes. *Bull. Soc. Chim. Fr.* **1993,** *130*, 25-31.
45. Pötschke, N.; Nieger, M.; Niecke, E., Crystal Structure of 1,1,1,3,3,3-Hexafluoro-2-propanyloxy-(2,4,6-tri-*tert*-butylphenylimino)phosphine. *Acta Chem. Scand.* **1997,** *51*, 337-339.
46. Kuprat, M.; Kuzora, R.; Lehmann, M.; Schulz, A.; Villinger, A.; Wustrack, R., Silver tetrakis(hexafluoroisopropoxy)aluminate as hexafluoroisopropyl transfer reagent for the chlorine/hexafluoroisopropyl exchange in imino phosphanes. *J. Organomet. Chem.* **2010,** *695*, 1006-1011.
47. Chernega, A. N.; Antipin, M. Y.; Struchkov, Y. T.; Ruban, A. V.; Romanenko, V. D., Structure of organophosphorus compounds. Part XLII. The molecular structure of the 2,6-di-*tert*-butyl-4-methylphenyl ester of *N*-[2,4,6-tri(*tert*-butyl)-phenyl]phosphenimidous acid. *J. Struct. Chem.* **1989,** *30*, 957-962.
48. Chernega, A. N.; Rusanov, É. B.; Ruban, A. V.; Romanenko, V. D., Molecular structure of $\sigma^3\lambda^5$. *J. Struct. Chem.* **1991,** *32*, 718-728.
49. Pötschke, N.; Barion, D.; Nieger, M.; Niecke, E., Chirale Iminophosphane durch Reaktion von Lithiumalkoholaten mit Chlor-(2,4,6-tri-*tert.*-butylphenylimino)phosphan. *Tetrahedron* **1995,** *51*, 8993-8996.
50. Chernega, A. N.; Romanenko, V. D., Molecular structure of the (−)menthyl ester of *N*-(2,4,6-tri-*tert*-butylphenyl)imidophosphinous acid. *J. Struct. Chem.* **1996,** *37*, 364-366.

TOC: